Preprints of the 19th World Congress
The International Federation of Automatic Control
Cape Town, South Africa. August 24-29, 2014

Control of Strip Tension in a Rolling Mill Based on Loopers and Impedance Control

A. Steinboeck G. Mühlberger A. Kugi

Automation and Control Institute, Vienna University of Technology,
Gußhausstraße 27-29, 1040 Vienna, Austria
(e-mail: andreas.steinboeck@tuwien.ac.at)

Abstract: A mathematical model of a strip-looper system of a hot strip tandem rolling mill is developed using Hamilton's principle and the Galerkin weighted residual method. Several nonlinearities are considered and the effects of bending and dynamic forces on the accuracy of the model are studied. Based on the model, an estimator for the strip tension is proposed. Finally, an impedance controller for the strip tension and the looper position is designed. It can be used in the whole operating range of the system, which is also demonstrated in a simulation scenario.

Keywords: Nonlinear systems, Impedance control, Distributed parameter system, Hamilton's principle, Steel industry, Tandem rolling mill, Looper control, Strip tension control.

1. INTRODUCTION

In the metals industry, tandem hot strip rolling mills are used for rolling out thick semi-finished products, e. g., slabs, to thinner flat products. The product, which is often referred to as strip, is clamped in each mill stand of the rolling mill train (cf. Fig. 1). As longitudinal tensile stresses in the strip have a significant influence on the plastic material flow in the roll gaps, accurate control of these stresses is important for the quality of the strip, including its shape and thickness. Well-tried state-of-the-art solutions for controlling the strip tension are so-called looper rolls (cf. Choi et al., 2007b; Price, 1973) located between the mill stands as shown in Fig. 1.

The idea of operating hot-rolling mills without loopers has been analyzed by Katori et al. (1999); Kim et al. (2005); and Li and Janabi-Sharifi (2009). However, looperless tension control is a delicate task due to the high tensile stiffness of the strip, the high inertia of the drive trains, the required high torques, and the required fast response time of the drive motors. These challenges have yet prevented the advent of looperless operation of conventional hot rolling mills. We thus consider tandem rolling mills equipped with loopers in this paper.

Due to their easy setup, PI force controllers are still the most prevalent controllers for the position of looper rolls (Choi et al., 2007b). More advanced control systems use tension meters (Zhao et al., 2008) to measure the current strip tension. Choi et al. (2007a) advocate the use of linear model predictive control (MPC) for loopers and strip tension as this control approach facilitates a systematic consideration of constraints and the multiple interactions between loopers and mill stands. Choi et al. (2007a) analyzed MPC formulations featuring robustness against disturbances with known stochastic characteristics. Nonlinear control concepts based on backstepping and sliding mode control were reported by Hesketh et al. (1998). Decoupling concepts for strip tension and looper dynamics were developed by Zhong and Wang (2011) based on feedback linearization and by Noh et al. (2012) based on a nonlinear disturbance observer.

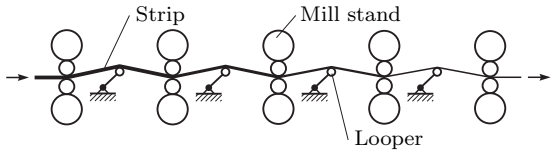

Fig. 1. Tandem rolling mill with five mill stands.

In more advanced multivariable control systems, the interaction between strip thickness, roll speed, roll gap dimensions, strip tension, and looper angle is systematically taken into account. Mathematical models that describe these interactions are typically derived by linearization at the respective operating point (Hearns et al., 2009; Obregón et al., 2010) or along an operating trajectory (Pittner and Simaan, 2010). Based on such models, the design of H_∞-controllers (Imanari et al., 1997) or linear-quadratic-regulator-type (LQR) controllers (Miura et al., 1993; Okada et al., 1998; Pittner and Simaan, 2010) for strip thickness, strip tension, and looper angle is common practice. A combined application of an LQR and a Kalman filter for state estimation was reported by Hearns et al. (2009). In (Okada et al., 1998), the interaction between mill stands is formally removed by state transformations. Jiao et al. (2011) developed a decentralized adaptive controller for strip thickness, strip tension, and looper dynamics based on a nonlinear model.

The main loads of the looper are its own weight, the weight of the strip, and the forces due to the tension forces and the bending moment in the strip. Cheng et al. (2006) argue that, at least for thin strips, the load due to the bending stiffness of the strip is negligible compared to the other three effects. Pittner and Simaan (2010) use a model that takes the bending moment of the strip into account but it

is not clear how this moment is computed. Apart from the work of Pittner and Simaan (2010), all above mentioned controllers are based on models that ignore the bending stiffness of the strip. It should thus be quantitatively analyzed for which looper geometries and strip properties this modeling assumption is tenable.

Some tandem rolling mills operate with an endless strip (cf. Takano et al., 1997), which implies that the semi-finished products have to be joined by welding before rolling and afterwards cut into lengths that can be coiled. However, it is more common that each product is individually rolled without welding. In this case, there is a threading and an unthreading phase of the strip where the looper has to be at the pass line level (rest position). After the threading phase, the looper is quickly raised to its upper position (working position), where it controls the strip tension. Many published looper control systems use force control only for the working position and position control in any other case. This standard strategy requires to switch between force and position control, which may entail a jerky response of the closed loop. Impedance control is a potential solution to avoid such problems. It was successfully applied to a looper system by Asano et al. (2000). They used a linear SISO model of the looper being in its working position, i. e., the threading and unthreading phase of the strip were not considered.

In view of the existing solutions for looper control, the objectives of the current paper are as follows:

(a) Explore whether the bending stiffness, the plastic deformation, and the dynamic forces of the strip should be captured by an accurate mathematical model of the looper. Determine whether the system exhibits significant nonlinearities.
(b) Design an estimator for the strip tension.
(c) Design a controller that is capable of controlling the looper in the whole operating range, i. e., in the working position and also for threading and unthreading of the strip below the working position.

In Section 2, we develop a distributed parameter model of the strip-looper system and reduce it to a finite-dimensional state space representation. The model is then used in Section 3 to answer the questions raised in objective (a) and in Section 4 to propose an estimator for the strip tension. In Section 5, we design an impedance controller and demonstrate its usefulness by means of simulations.

2. MATHEMATICAL MODEL

2.1 Application of Hamilton's Principle

Fig. 2 shows the geometry of the looper, i. e., a rigid body, and the elastic strip. Many authors in the field approximate the strip with two straight lines. In essence, however, the strip has a curved shape because it is subject to a bending moment. An accurate computation of this moment requires the solution of a boundary value problem. We apply Hamilton's principle (cf. Reddy, 2002) for deriving this boundary value problem.

As indicated in Fig. 2, $w = w(x,t)$ is the vertical displacement of the strip, $v = v(t)$ is its given longitudinal velocity,

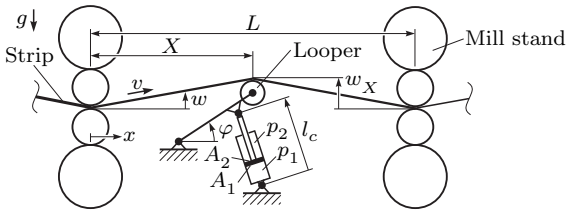

Fig. 2. Geometry of strip and looper in working position.

which varies just slowly, and $\varphi = \varphi(t)$ is the angular position of the looper. In the following, $\dot{(\cdot)} = \partial(\cdot)/\partial t$ denotes the time derivative and $(\cdot)' = \partial(\cdot)/\partial x$ the derivative with respect to the spatial coordinate x. Later, we will use the same symbols for total derivatives. Wherever confusion is ruled out, the arguments x and t are omitted. The kinetic energy of the system reads as

$$K = \frac{1}{2}\rho \int_0^L (\dot{w} + v w')^2 \mathrm{d}x + \frac{1}{2}\Theta \dot{\varphi}^2,$$

where ρ is the mass of the strip per unit length, L is the horizontal distance between two mill stands, and Θ is the moment of inertia of the looper with respect to its pivot point. The potential energy follows in the form

$$V = \rho g \int_0^L w \mathrm{d}x + mgh + F\Delta l + \frac{1}{2}EA \int_0^L \varepsilon^2 \mathrm{d}x. \quad (1)$$

The looper has the mass m and its center of gravity has the vertical position h. The infinitesimal strip element shown in Fig. 3 has the current length $\mathrm{d}s = \sqrt{1 + w'^2}\mathrm{d}x \approx (1 + w'^2/2)\mathrm{d}x$. The actual strip length thus follows in the form $l = L + \Delta l$ with the surplus strip length $\Delta l = \int_0^L w'^2 \mathrm{d}x/2$.

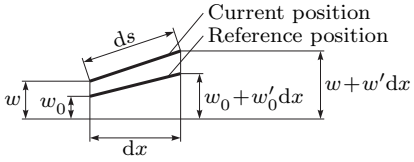

Fig. 3. Infinitesimal element of the strip.

Generally, the tensile force F applied to the strip at the mill stands is non-conservative. In this work, two special cases are considered: Either F is constant (for slow and large changes of looper position, e. g., quasi steady-state movement from rest position to working position or vice versa) or Δl is constant (for fast but small changes of F, e. g., looper is in working position). Hence, the third term in (1) represents the potential energy associated with F. The two special cases cover the whole dynamic range of the system because significant long-term changes of F are prevented by control and significant short-term changes of Δl are prevented by the high inertia of the rolls and their drive trains.

The last term in (1) is the strain energy corresponding to pure longitudinal stretch of the strip. E is the Young's modulus, A is the cross sectional area of the strip, and ε is the local mean longitudinal strain in the strip. The strain energy due to longitudinal stretch is constant if F is constant. Consider the following scenario: Some looper controller ensures that $F = F_0$ is held constant while the surplus strip length Δl is gradually increased

by controlling the differential speed of the adjacent mill stands. In this way, the looper moves from its rest position to its working position, where it stops as the mill speeds are synchronized. A (loaded) steady state is reached and the resulting shape $w_0(x)$ of the strip is used as a reference for subsequent calculations. Despite the synchronized mill speeds, the actual strip length l may slowly change over time due to the stretch of the strip caused by variations of F. To compute ε and F, consider again the infinitesimal strip element $\mathrm{d}s$ shown in Fig. 3. Its length in the unloaded state is $\mathrm{d}s_0 \approx \mathrm{d}x/a$ with the abbreviation

$$a = \frac{1+\frac{F_0}{EA}}{1+\frac{w_0'^2}{2}}.$$

Consequently, we obtain the local strain value

$$\varepsilon = \frac{\mathrm{d}s}{\mathrm{d}s_0} - 1 = a\Big(1+\frac{w'^2}{2}\Big) - 1.$$

Using the length $\int_0^L a\mathrm{d}x$ of the unloaded strip yields

$$F = EA\bigg(\frac{l}{\int_0^L a^{-1}\mathrm{d}x} - 1\bigg). \tag{2}$$

The strain energy corresponding to bending deformations is generally non-conservative because of possible plastic deformations. The effect of the bending moment is captured by the first term of the following virtual work expression.

$$\delta W = -\int_0^L M\delta w''\mathrm{d}x + F_c\delta l_c \tag{3}$$

The bending moment M can be modeled as

$$M = \begin{cases} M_e & \text{if } \frac{Ed}{2}|w''-\kappa_0| \le \sigma_Y \\ M_{ep} & \text{else} \end{cases} \tag{4a}$$

with the purely elastic term

$$M_e = E\frac{bd^3}{12(1-\nu^2)}(w''-\kappa_0) \tag{4b}$$

and the elasto-plastic term

$$M_{ep} = \sigma_Y b\Big(\frac{d^2}{4} - \frac{\sigma_Y^2}{3(w''-\kappa_0)^2E^2}\Big)\frac{\operatorname{sign}(w''-\kappa_0)}{1-\nu^2}. \tag{4c}$$

Here, d is the thickness of the strip, b is its width, κ_0 is its curvature in the unloaded state, σ_Y is the uniaxial tensile yield strength, and ν is the Poisson's ratio. In (4c), we assumed ideal plastic behavior (no work hardening), a negligible influence of F, a uniaxial stress state, and a bending stiffness that is amplified by the factor $1/(1-\nu^2)$ to capture the effect of inhibited lateral strains. Strictly speaking, we would need to consider a plane stress state, a yield criterion, and numeric integration of the plastic strains according to a flow rule, e. g., the Levy-Mises flow rule. However, it can be easily verified that (4c) is a tenable approximation of this more accurate approach. The initial curvature κ_0 can be computed and updated at the end of each section where the strip is plastically bent, that is after each roll gap and after the looper roll.

The term $F_c\delta l_c$ in (3) represents the virtual work of the hydraulic cylinder that lifts the looper. F_c is the effective force of the cylinder and l_c is its current length (cf. Fig. 2).

For simplicity, we assume that the strip touches the looper roll at its upper vertex, which is at the position $x = X(t)$. As can be inferred from Fig. 2, the quantities $X(t)$, $w(X,t)$, $h(t)$, $l_c(t)$, and $\varphi(t)$ are coupled by straightforward geometric relations. Henceforth, we will use the abbreviation $w_X = w(X,t)$ to parameterize the other variables.

The strip does not have kinks or folds and it is vertically clamped in the roll gaps. Hence, we have the geometric boundary conditions

$$w(0,t) = 0, \qquad w'(0,t) = 0, \tag{5a}$$
$$w(L,t) = 0, \qquad w'(L,t) = 0, \tag{5b}$$
$$w(X^-,t) = w(X^+,t), \qquad w'(X^-,t) = w'(X^+,t), \tag{5c}$$

where X^- identifies the left-hand limit and X^+ the right-hand limit of the respective function at the position X.

According to Hamilton's principle,

$$\int_{t_0}^{t_1} \delta K - \delta V + \delta W\mathrm{d}t = 0, \tag{6}$$

where t_0 and t_1 are two arbitrary points in time. Integrating (6) by parts, using (5), and considering that $\dot v$ is negligibly small and that δw can be an arbitrary kinematically admissible variation, we obtain

$$\rho(\ddot w + 2v\dot w' + v^2w'' + g) - Nw'' + M'' = 0 \tag{7a}$$

and the additional boundary conditions

$$\begin{aligned} -\Theta\Big(\frac{\mathrm{d}^2\varphi}{\mathrm{d}w_X^2}\dot w_X^2 + \frac{\mathrm{d}\varphi}{\mathrm{d}w_X}\ddot w_X\Big)\frac{\mathrm{d}\varphi}{\mathrm{d}w_X} - mg\frac{\mathrm{d}h}{\mathrm{d}w_X} \\ + M'(X^-) - M'(X^+) + F_c\frac{\mathrm{d}l_c}{\mathrm{d}w_X} = 0 \end{aligned} \tag{7b}$$

$$M(X^+) - M(X^-) = 0, \tag{7c}$$

with $N = F_0$ if the looper is below its working position or

$$N = EA\Big(a'(a(w'^2+2)-1)\frac{w'}{w''} + a\Big(a\Big(\frac{3}{2}w'^2+1\Big)-1\Big)\Big) \tag{7d}$$

if the looper is in its working position.

2.2 Application of Galerkin Weighted Residual Method

For spatial discretization of (7a), we use the Galerkin weighted residual method (Zienkiewicz et al., 2013). The solution is thus approximated in the form

$$w(x,t) = w_X(t)\hat w(x) \tag{8}$$

with the base function $\hat w(x) = w_0(x)/w_0(X)$, where $w_0(x)$ is the steady-state solution of (5) and (7) at the respective operating point. It is numerically computed from (5) and (7a)–(7c) with $N = F_0$, $v > 0$, $\dot w = 0$, $\ddot w = 0$, and $\dot w' = 0$.

Consider that the operator $\operatorname{lhs}[\cdot]$ extracts the left-hand side of an equation. Hence, the Galerkin method yields

$$\int_0^L \operatorname{lhs}[(7a)]\hat w(x)\mathrm{d}x + \operatorname{lhs}[(7b)] = 0, \tag{9}$$

which is evaluated twice for $N = F_0$ and N from (7d). All boundary conditions that are not included in (9) are automatically satisfied by the approximation (8).

2.3 Hydraulic Actuation

The effective force F_c applied by the hydraulic cylinder to the looper can be modeled in the form

$$F_c = p_1A_1 - p_2A_2 - F_f, \tag{10}$$

where p_1 and p_2 are the pressures in the bottom chamber and in the piston rod side chamber, respectively. A_1 and A_2 are the cross-sectional areas of these chambers, and

$$F_f = \operatorname{sign}(\dot l_c)\big(a_1 + a_2\mathrm{e}^{a_3|\dot l_c|} + a_4(p_1-p_2) + a_5(p_1+p_2)\big) \tag{11}$$

models the friction forces in the cylinder and the pivot point of the looper. The parameters a_i $(i = 1, \ldots, 5)$ have to be identified based on measurements. The pressures p_1 and p_2 are modeled by

$$\dot{p}_1 = \frac{\beta}{V_1 + A_1 l_c}(q_1 - A_1 \dot{l}_c) \tag{12a}$$

$$\dot{p}_2 = \frac{\beta}{V_2 - A_2 l_c}(q_2 + A_2 \dot{l}_c), \tag{12b}$$

where β is the bulk modulus of the hydraulic oil, V_1 and V_2 are offset volumes of the two cylinder chambers, and q_1 and q_2 are volume flows into these chambers. The volume flows are controlled by an electro-hydraulic servo valve, which is modeled based on the classic orifice equation. This yields

$$q_1 = s \begin{cases} c_s \operatorname{sign}(p_s - p_1)\sqrt{p_s - p_1} & \text{if } s > 0 \\ c_r \operatorname{sign}(p_1 - p_r)\sqrt{p_1 - p_r} & \text{else} \end{cases} \tag{13a}$$

$$q_2 = s \begin{cases} c_r \operatorname{sign}(p_2 - p_r)\sqrt{p_2 - p_r} & \text{if } s > 0 \\ c_s \operatorname{sign}(p_s - p_2)\sqrt{p_s - p_2} & \text{else} \end{cases} \tag{13b}$$

with the supply pressure p_s, the pressure p_r in the oil reservoir, the spool displacement s, and the constants c_s and c_r.

2.4 Assembled System

Based on (9)–(13), we obtain the dynamical model

$$\dot{\boldsymbol{x}} = \boldsymbol{f}(\boldsymbol{x}, u, t) \tag{14}$$

with the state $\boldsymbol{x} = [w_X, \dot{w}_X, p_1, p_2]^T$ and the input $u = s$. It is time-variant because different strips are rolled, the looper changes its operating point, and it moves to the rest position between the roll passes. The system is significantly nonlinear (cf. (7) and (10)–(13)). Hence, it is not recommendable to use a linearized model for controlling the looper in the whole operating range.

3. ANALYSIS

Based on the developed model, we study the influence of bending and dynamic forces on the steady-state shape of the strip. The analysis is done for the hot strip finishing mill of voestalpine Stahl GmbH, Linz, Austria. We consider two scenarios: a strip with thickness $d = 2\,\text{mm}$ and another strip with thickness $d = 15\,\text{mm}$. Both strips have the width $b = 1\,\text{m}$, the yield strength $\sigma_Y = 129.2\,\text{MPa}$, the Young's modulus $E = 70\,000\,\text{MPa}$, and the Poisson's ratio $\nu = 0.3$. For better comparison, the rolling velocity $v = 10\,\text{m/s}$, the strip tension 10 MPa, and the looper height $w_X = 244\,\text{mm}$ are identically used for both strips. The resulting steady-state shapes of the strips are shown in Fig. 4. The result confirms that a higher bending stiffness causes smaller curvatures of the strip near the looper roll.

Fig. 4. Shape of strip in working position.

Table 1. Errors of w_X and F_c if bending and dynamic forces are neglected.

Effect	Max. abs. error of w_X for strip with thickness $d = 2\,\text{mm}$	$d = 15\,\text{mm}$	Relative error of F_c for strip with thickness $d = 2\,\text{mm}$	$d = 15\,\text{mm}$
No bending stiffness, $M = 0$	4.8 mm	26.8 mm	0.2 %	−19.4 %
No plastic deformation, $M = M_e$	0.2 mm	3.3 mm	1.3 %	3.0 %
No dynamic forces, $v = 0$	0.7 mm	1.2 mm	2.3 %	5.5 %
Triangular approximation	9.2 mm	21.1 mm	2.1 %	−15.7 %

The results of the mathematical model with certain effects being masked out are summarized in Table 1.

To consider a bending stiffness of 0, we use $M = 0$. To neglect plastic deformations, we use $M = M_e$ instead of (4a). The influence of dynamic forces (Coriolis and centrifugal forces) is ignored if we use $v = 0$. The last line of Table 1 contains results for the triangular approximation that is used in many looper models (cf. Cheng et al., 2006; Noh et al., 2012; Price, 1973; Zhong and Wang, 2011). With this approximation, the strip is represented by two straight lines, which yields

$$-\Theta\Big(\frac{\mathrm{d}^2\varphi}{\mathrm{d}w_X^2}\dot{w}_X^2 + \frac{\mathrm{d}\varphi}{\mathrm{d}w_X}\ddot{w}_X\Big)\frac{\mathrm{d}\varphi}{\mathrm{d}w_X} - mg\frac{\mathrm{d}h}{\mathrm{d}w_X} - \frac{1}{2}\rho L g$$
$$-F\Big(\frac{w_X}{\sqrt{X^2 + w_X^2}} + \frac{w_X}{\sqrt{(L-X)^2 + w_X^2}}\Big) + F_c\frac{\mathrm{d}l_c}{\mathrm{d}w_X} = 0$$

instead of (7). Table 1 shows that the errors entailed by the applied approximations are larger for thicker strips. Especially, neglecting the bending stiffness or using the triangular approximation can cause significant errors.

4. ESTIMATION OF STRIP TENSION

The tensile stress in the strip is an important production parameter, which directly influences the material flow in the roll gap and also the structure of the material. Without special devices like tension-meters (cf. Zhao et al., 2008), the tensile stress in the strip cannot be directly measured. Computing the tensile stress based on (2) is usually also not feasible because w is not measured and l is thus unknown. However, the tensile stress can be estimated if the pressure values p_1 and p_2 and the length l_c of the hydraulic cylinder are measured. The following describes how such an online estimation can be realized based on the model developed in Section 2.

From the measurement of l_c, we can compute w_X. Consequently, the velocity $\dot{w}_X$ and the acceleration $\ddot{w}_X$ can be estimated. Together with the measured values for p_1 and p_2, these values are inserted into the second row of (14) (differential equation for $\dot{w}_X$) specialized for the current operating point. The result is a simple algebraic equation for F so that the strip tension F/A can be easily computed. If the estimations of $\dot{w}_X$ and $\ddot{w}_X$ are impaired by noise, it is often tenable to neglect the associated dynamic forces in (14), which means that a steady-state scenario is assumed. Then, there is a static relation between w_X, F_c, and F, which can be numerically computed and stored in a look-up table for rapid online evaluation.

5. IMPEDANCE CONTROL

5.1 Control Structure

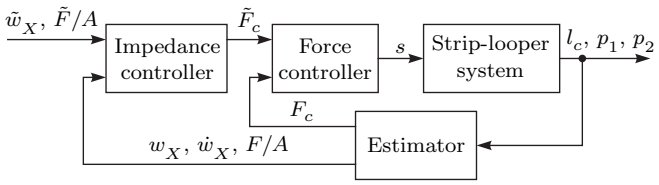

Fig. 5. Cascade control structure.

We design a controller that can be used at any operating point of the strip-looper system. To circumvent the problems of pure position control (possible overloads) and pure force control (possible large position deviations), impedance control is used for the considered control task. The cascade control structure, which is outlined in Fig. 5, uses a subordinate force controller for F_c based on input/state linearization of the hydraulic model (cf. Kugi, 2001). The resulting linear system is stabilized by PI-control. For the design of the superordinate impedance controller, we can thus use the dynamic model

$$\dot{\boldsymbol{x}}_1 = \boldsymbol{f}_1(\boldsymbol{x}_1, u_1, t) \tag{15}$$

(cf. (14)) with the state $\boldsymbol{x}_1 = [w_X, \dot{w}_X]^T$. The second line of (15) can always be inverted to obtain the input

$$u_1 = F_c = f_{12}^{-1}(\boldsymbol{x}_1, \ddot{w}_X, t). \tag{16}$$

5.2 Control Law

Consider a desired looper position $\tilde{w}_X$ and a desired strip tension $\tilde{F}/A$. These two values also determine the current operating point of the looper. Note that only the system, where the mill speeds are synchronized and where the looper is in its working position (N from (7d)) is considered for control design because otherwise $F = F_0$ would be constant anyway. Since the operating point may change over time, (15) and (16) are time-varying. However, this time dependence is small because $\tilde{w}_X$, $\tilde{F}/A$, and other parameters defining the operating point, e. g., v, change just slowly. Consequently, we neglect the time dependence of (15), (16), $\tilde{w}_X$, and $\tilde{F}/A$ for control design.

Impedance control means that the controller imitates a user-defined dynamic relation between the control errors in terms of position and force. Our user-defined dynamic system has the form

$$C\ddot{w}_X + D\dot{w}_X + S(w_X - \tilde{w}_X) = -\frac{F - \tilde{F}}{A} \tag{17}$$

with the position control error $\Delta w_X = w_X - \tilde{w}_X$, the tension control error $(F - \tilde{F})/A$, and appropriately chosen positive constants C and D. The monotonously non-decreasing stiffness function

$$S(\Delta w_X) = S_1 \Delta w_X + S_2 \operatorname{atanh}\Big(\frac{\Delta w_X^3}{\Delta w_{X,max}^3}\Big),$$

with constants $S_1 > 0$ and $S_2 > 0$ determines the steady-state control error. In fact, it limits the steady-state position error in the form $|\bar{w}_X - \tilde{w}_X| < \Delta w_{X,max}$, where a bar is used to label steady-state values. Alternatively, we could use the stiffness function $S(\Delta w_X) = \tanh(S_3 \Delta w_X)\Delta F_{max}/A$ with the constant $S_3 > 0$, which limits the steady-state tension control error in the form $|\bar{F} - \tilde{F}|/A < \Delta F_{max}/A$.

From (16) and (17), we obtain the control law

$$\tilde{F}_c = f_{12}^{-1}\Big(\boldsymbol{x}_1, -\frac{D\dot{w}_X + S(w_X - \tilde{w}_X) + (F - \tilde{F})/A}{C}, t\Big).$$

The current tensile force F is monotonously increasing with respect to w_X and can be estimated as described in Section 4. For the following stability analysis, however, consider that $F = F(w_X)$ is computed by means of (2).

5.3 Stability Analysis

According to (17), the steady-state position $\bar{w}_X$ of the closed-loop controlled system is defined by

$$S(\bar{w}_X - \tilde{w}_X) = -\frac{F(\bar{w}_X) - \tilde{F}}{A}.$$

Based on the positive definite Lyapunov function

$$U(e, \dot{w}_X) = \frac{C}{2}\dot{w}_X^2 + \int_{\bar{w}_X}^{e+\bar{w}_X} S(\xi - \tilde{w}_X) + \frac{F(\xi) - \tilde{F}}{A} \mathrm{d}\xi,$$

with $e = w_X - \bar{w}_X$, and its time derivative

$$\dot{U}(e, \dot{w}_X) = -D\dot{w}_X^2 \leq 0,$$

where we used (17), it follows from LaSalle's principle (Vidyasagar, 1992) that the steady state $\bar{\boldsymbol{x}}_1 = [\bar{w}_X, 0]^T$ is asymptotically stable. This holds in the whole operating range of the system.

5.4 Simulation

The closed-loop behavior of the developed impedance controller is studied by means of simulations. The simulation environment is structured in the same way as shown in Fig. 5 with the real strip-looper system being emulated by (14). To test the robustness of the system, the signals p_1 and p_2 are degraded by measurement noise and the signal l_c is quantized. The same two scenarios as defined in Section 3 are used in the simulation, i. e., the strip has a thickness of $d = 2\,\mathrm{mm}$ or $d = 15\,\mathrm{mm}$.

The differential speed of the rolling mills is controlled so that the surplus strip length Δl follows the trajectory given in Fig. 6a. This is the typical shape of Δl after the strip has been threaded. Consequently, the looper has to move from the rest position with $w_X = 0\,\mathrm{mm}$ to a final working position, while the strip tension should be kept at the constant desired value $\tilde{F}/A = 10\,\mathrm{MPa}$. Using the steady-state solution of (5) and (7a)–(7c) with $N = \tilde{F}$, we can compute $\tilde{w}_X$ corresponding to Δl. Both the desired signal $\tilde{w}_X$ and the closed-loop controlled signal w_X are shown in Fig. 6b. Fig. 6c shows that the strip tension F/A agrees well with its desired value $\tilde{F}/A$. The reverse transition from the working to the rest position works fairly the same way and with the same control accuracy.

ACKNOWLEDGEMENTS

The authors gratefully acknowledge useful support by voestalpine Stahl GmbH, Linz, Austria. The first author gratefully acknowledges financial support provided by the

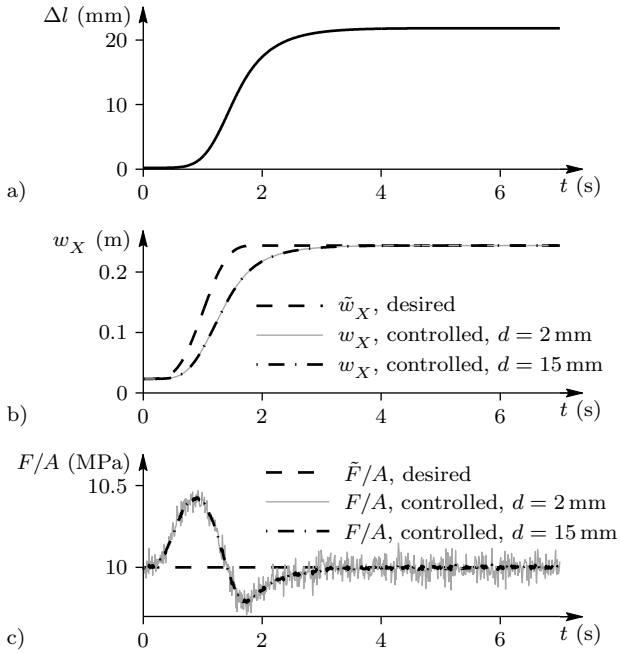

Fig. 6. Closed-loop behavior for transition from rest to working position, a) surplus strip length, b) position of looper, c) strip tension.

Austrian Academy of Sciences in the form of an APART-fellowship at the Automation and Control Institute of Vienna University of Technology.

REFERENCES

Asano, K., Yamamoto, K., Kawase, T., and Nomura, N. (2000). Hot strip mill tension-looper control based on decentralization and coordination. *Control Engineering Practice*, 8(3), 337–344.

Cheng, C.C., Hsu, L.Y., Hsu, Y.L., and Chen, Z.S. (2006). Precise looper simulation for hot strip mills using an auto-tuning approach. *The International Journal of Advanced Manufacturing Technology*, 27(5-6), 481–487.

Choi, I., Rossiter, A., and Fleming, P. (2007a). Effectiveness of MPC algorithms for hot rolling mills in the presence of disturbances. *Proceedings of the American Control Conference, New York, USA*, 4118–4123.

Choi, I., Rossiter, J., and Fleming, P. (2007b). Looper and tension control in hot rolling mills: A survey. *Journal of Process Control*, 17(6), 509–521.

Hearns, G., Bilkhu, T., and Reeve, P. (2009). *Flat-Rolled Steel Processes: Advanced Technologies*, chapter Multivariable Hot Strip Mill Control, 209–218. CRC Press, Boca Raton.

Hesketh, T., Jiang, Y., Clements, D., Butler, D., and Van der Laan, R. (1998). Controller design for hot strip finishing mills. *IEEE Transactions on Control Systems Technology*, 6(2), 208–219.

Imanari, H., Morimatsu, Y., Sekiguchi, K., Ezure, H., Matuoka, R., Tokuda, A., and Otobe, H. (1997). Looper H-infinity control for hot-strip mills. *IEEE Transactions on Industry Applications*, 33(3), 790–796.

Jiao, X.H., Shao, L.P., and Peng, Y. (2011). Adaptive coordinated control for hot strip finishing mills. *International Journal of Iron and Steel Research*, 18(4), 36–43.

Katori, H., Hirayama, R., Ueyama, T., and Furuta, K. (1999). On the possibility of looperless rolling on hot rolling process. In *Proceedings of the IEEE Conference on Control Applications*, volume 1, 18–22.

Kim, J., Shim, J., Han, D., Park, C., Park, H., and Lee, S. (2005). A study of tension control in looperless hot rolling process using SVR. In *Proceedings of ICMIT 2005: Control Systems and Robotics, Chongqing, China*, 60420Z 1–6.

Kugi, A. (2001). *Non-linear Control Based on Physical Models*. Number 260 in Lecture Notes in Control and Information Sciences. Springer, London.

Li, G. and Janabi-Sharifi, F. (2009). Fuzzy looperless tension control for hot strip rolling. *Fuzzy Sets and Systems*, 160(4), 521–536.

Miura, H., Nakagawa, S., Fukushima, S., and Amasaki, J. (1993). Gauge and tension control system for hot strip finishing mill. In *Proceedings of the IECON '93 International Conference on Industrial Electronics, Control, and Instrumentation, Keisoku, Japan*, volume 1, 463–468.

Noh, I., Won, S., and Jang, Y. (2012). Non-interactive looper and strip tension control for hot finishing mill using nonlinear disturbance observer. *ISIJ International*, 52(6), 1092–1100.

Obregón, A., Mendiola, P., Evers, K., Cavazos, A., and Leduc, L. (2010). Linear multivariable dynamic model of a hot strip finishing mill. *Proceedings of the Institution of Mechanical Engineers. Part I: Journal of Systems and Control Engineering*, 224(8), 1007–1021.

Okada, M., Murayama, K., Urano, A., Iwasaki, Y., Kawano, A., and Shiomi, H. (1998). Optimal control system for hot strip finishing mill. *Control Engineering Practice*, 6(8), 1029–1034.

Pittner, J. and Simaan, M. (2010). A control method for improvement in the tandem hot metal strip rolling process. *Conference Record - IAS Annual Meeting (IEEE Industry Applications Society)*, 5615455, 1–8.

Price, J. (1973). The hot strip mill looper system. *IEEE Transactions on Industry Applications*, IA-9(5), 556–562.

Reddy, J. (2002). *Energy Principles and Variational Methods in Applied Mechanics*. Wiley, Hoboken, 2nd edition.

Takano, T., Matsuda, K., Moriya, S., Shibatomi, N., Mito, Y., and Hayashi, K. (1997). Endless hot strip rolling at Kawasaki Steel Chiba works. *Iron and Steel Engineer*, 74(2), 41–47.

Vidyasagar, M. (1992). *Nonlinear systems analysis*. Number 42 in Classics in Applied Mathematics. SIAM, Philadelphia, 2nd edition.

Zhao, X., Zhang, Z., Sun, Y., Wang, J., and Que, C. (2008). A contact-type tensionmeter for hot rolling mills. *Proceedings of SPIE - The International Society for Optical Engineering*, 7130, 71302R 1–6.

Zhong, Z. and Wang, J. (2011). Looper-tension almost disturbance decoupling control for hot strip finishing mill based on feedback linearization. *IEEE Transactions on Industrial Electronics*, 58(8), 3668–3679.

Zienkiewicz, O., Taylor, R., and Zhu, J. (2013). *The Finite Element Method: Its Basis and Fundamentals*. Elsevier, Amsterdam, 7th edition.